EPJ Web of Conferences **83**, 02016 (2015)
DOI: 10.1051/epjconf/20158302016

Protein and solvent dynamics of the water-soluble chlorophyll-binding protein (WSCP)

Leonid Rusevich[1], Jan Embs[2], Inga Bektas[3], Harald Paulsen[3], Gernot Renger[4] and Jörg Pieper[5,a]

[1]Institute of Physical Energetics, Riga, Latvia
[2]Paul-Scherrer Institute, Villigen, Switzerland
[3]Institute of General Botany, Johannes Gutenberg University Mainz, Germany
[4]Technical University, Max-Volmer-Laboratories for Biophysical Chemistry, Berlin, Germany
[5]Institute of Physics, University of Tartu, Tartu, Estonia

Abstract. This study presents quasielastic neutron scattering data of the water-soluble chlorophyll-binding protein (WSCP) and the corresponding buffer solution at room temperature. The contributions of protein and buffer solution to the overall scattering are carefully separated. Otherwise, the fast water dynamics dominating the buffer contribution is likely to mask the slow protein dynamics. In the case of WSCP, the protein scattering can be described by two contributions: i) internal protein dynamics represented by a diffusion in a sphere with an average radius of 2.7 Å and ii) global (Brownian) diffusion of the WSCP macromolecule with an upper limit for the translational diffusion coefficient of $9.4 \cdot 10^{-7}$ cm^2/s.

1. Introduction

Protein dynamics due to stochastic structural fluctuations of small molecular subgroups on the picosecond time scale has been shown to play an important role in physiological processes in nature. Prominent examples for such dynamics-function correlations include proton transfer in bacteriorhodopsin of *halobacterium salinarum* [1,2], ligand binding to myoglobin [3], and photosynthetic electron transfer in plant photosystem II [4]. In the case of photosystem II membrane fragments of green plants, quasielastic neutron scattering (QENS) has established that the onset of diffusive molecular motions at ∼240 K [4], and at a relative humidity of ∼45% [5] is strictly correlated with the temperature- and hydration-dependent electron transfer efficiency from an electron donor referred to as Q_A^- to a transiently bound acceptor molecule named Q_B. Such a characteristic dependence of a functional process on temperature and hydration may indicate a crucial role of molecular dynamics in the underlying molecular mechanism [4,6].

Photosynthetic systems typically exhibit a high degree of complexity and bind a large number of pigment molecules or other functionally active co-factors. Therefore, it is often difficult to investigate specific pigment-protein interactions in such complex systems. In this regard, WSCP has recently been established as a minimal, but naturally abundant model system for photosynthetic pigment-protein complexes [7], although its own particular function is not yet clarified.

WSCP can be isolated from various plants and distinguished according to its response to illumination. While Class-I WSCP exhibits a spectral shift upon excitation, no photoconversion is observed for class-II (for a review see [8]). Class-II WSCPs are water-soluble and possess a molecular weight of about 20 kDa. Up to now, a crystal structure obtained by X-ray diffraction is available only for WSCP from *Lepidium virginicum* [9]. However, all class-II WSCPs occur in tetrameric form binding 1–4 chlorophyll molecules. A recombinant type of WSCP from cauliflower was found to contain 2 chlorophylls (class-IIa), while WSCP from *Lepidium virginicum* binds 4 chlorophylls per tetramer (class-IIb). Recombinant class-IIa WSCP binding only two chlorophylls has been used to investigate pigment-protein interactions and excitation energy transfer by a number of spectroscopic techniques including time-resolved absorption and fluorescence experiments, spectral line-narrowing and 2D electronic spectroscopy [10–14].

However, a direct investigation of WSCP protein dynamics by QENS is so far lacking. As a complicating factor for such studies, a significant solvent contribution to the overall scattering intensity can be expected as observed before for the antenna complex LHC II [15] and for the bacterial reaction center [16,17]. In the present study we address this problem by QENS experiments on WSCP and on the corresponding buffer solution at room temperature. We conclude that the contribution of protein scattering can be reliably separated and analyzed in terms of internal dynamics and global (Brownian) diffusion.

2. Materials and methods

WSCP protein dynamics on the picosecond timescale was investigated by QENS experiments using the time-of-flight spectrometer FOCUS at the Paul-Scherrer institute in Villigen, Switzerland. The measurements were performed with an incident neutron wavelength of 5 Å, an elastic

[a] Corresponding author: pieper@ut.ee

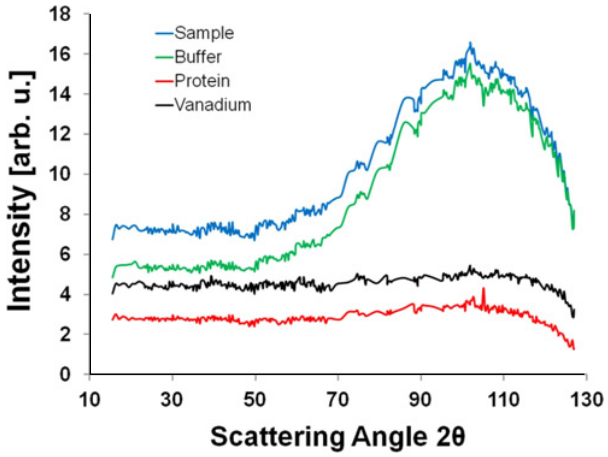

Figure 1. Angle spectra of sample solution (blue line), buffer (green line), vanadium (black line), and WSCP only (denoted as protein, red line) at 300 K.

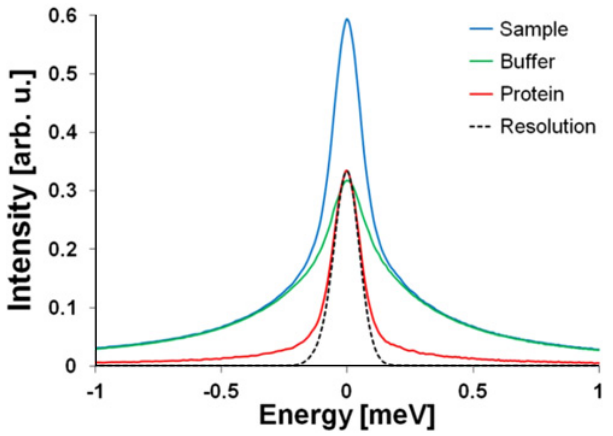

Figure 2. QENS spectra of WSCP in buffer solution (blue line), buffer (green line), resolution function (black dotted line), and the difference spectrum corresponding to WSCP (red line) possibly including bound hydration water. Data were obtained with a neutron wavelength of 5 Å and an elastic resolution of 0.123 meV at 300 K. Data shown are averaged over all scattering angles resulting in $Q = 1.46\,\text{Å}^{-1}$.

energy resolution ΔE of 0.123 meV and a scattering vector Q range of 0.33–2.25 Å^{-1}. The data were corrected for empty cell contribution, normalized and converted to energy transfer scale using the program package DAVE [18].

The sample preparation was adapted to QENS experiments. Briefly, recombinant WSCP from cauliflower (*Brassica oleracea var. botrytis*) was expressed as previously described [11] and reconstituted with purified chlorophyll *a* and chlorophyll *b* at a chlorophyll *a*/*b* ratio of 2.7:1. Finally, WSCP was diluted in a buffer solution containing 300 mM Imidazole, 20 mM NaP (pD = 7.5), and D_2O in order to minimize the solvent scattering. The protein concentration of the WSCP sample was about 80 mg/ml in a total volume of 2 ml. A similar amount of buffer was used for comparative measurements.

3. Results and discussion

Before discussing QENS spectra of WSCP, the contributions of protein (WSCP) and buffer solution to the overall scattering have to be carefully separated. In this regard, it is instructive to inspect the angle spectra of sample and buffer solution as well as that of a vanadium standard shown in Fig. 1. The sample solution exhibits an intense correlation peak at 2θ of about 95° that is absent in the incoherently scattering vanadium standard. The same correlation peak is visible in the angle spectrum of the buffer solution so that it can be mainly attributed to the coherent scattering of D_2O. Generally, the protein contribution can be derived by the relation

$$I_{\text{protein}} = I_{\text{sample}} - k \cdot I_{\text{buffer}}, \qquad (1)$$

where k is a scaling factor accounting for the buffer contribution to the total sample scattering. It is possible to rewrite (1) specifying coherent (I_{coh}) and incoherent (I_{inc}) contributions:

$$I_{sample,coh} + I_{sample,inc} = I_{protein} + k \cdot (I_{buffer,coh} + I_{buffer,inc}). \qquad (2)$$

Furthermore, it can be assumed that scattering of protein is almost entirely incoherent. Gaspar et al. [19] investigated the coherent and incoherent scattering of proteins by polarization analysis and found an incoherent scattering fraction of about 90 percent in completely dry myoglobin. Then, considering only the coherent part in (4), it follows that $I_{sample,coh} = k \cdot I_{buffer,coh}$ so that k can be determined as the ratio of the coherent scattering contributions of sample and buffer, represented here by the intensities of the correlation peak visible in Fig. 1. Once k is known, the protein contribution can be derived from (1). The resulting WSCP angle spectrum is also shown in Fig. 1.

A comparison of the angle spectra of vanadium and the WSCP in Fig. 1 reveals that these spectra are quite similar confirming incoherent nature of WSCP scattering.

Figure 2 shows the QENS spectra for the sample (black dotted line) and buffer solution (green line) as well as the resulting difference spectrum (red line) at room temperature, which correspond to the angle spectra shown in Fig. 1. The difference spectrum accounts for WSCP and its hydration shell of tightly bound water not reflected by buffer dynamics. A comparison of the data reveals that the dynamics of WSCP and of the buffer are essentially different. Qualitatively, it appears that the broad buffer spectrum is dominated by the fast diffusion of D_2O, while the narrower WSCP spectrum corresponds to slower dynamics. The buffer scattering constitutes a large part of the QENS spectrum of the sample (WSCP in buffer solution) and would largely obscure the protein scattering if the two contributions could not be reliably separated. This observation underlines that efforts to suppress the buffer scattering are of great importance when investigating proteins in solution.

In what follows, we will discuss the QENS spectrum of WSCP as derived above (see Fig. 2). For further analysis, the data were grouped into ten angle groups. Figure 3 shows QENS spectra of WSCP for three representative Q-values. As expected, the data reveal a

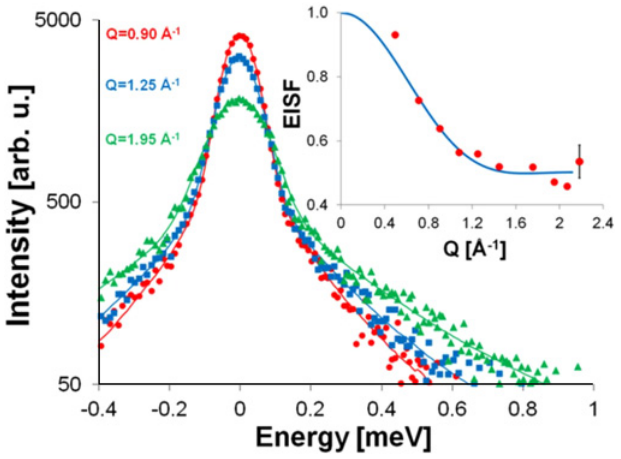

Figure 3. QENS spectra of the WSCP contribution for three representative Q-values (red, blue and green symbols, see labels for actual Q-value), obtained with a neutron wavelength of 5 Å and an elastic resolution width of 0.123 meV at 300 K. The full lines are fits by $S_{exp}(Q,\omega)$ (see text). The inset shows the resulting EISF as a function of Q (red points), a fit according to Eq. (3) (blue line) and a representative error bar.

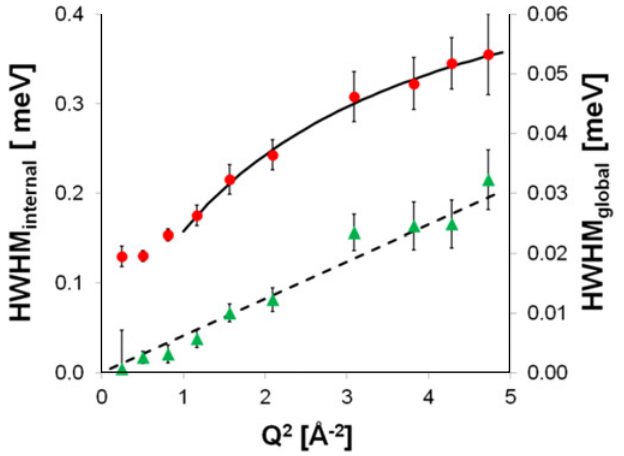

Figure 4. Widths (HWHM) of the Lorentzian contributions in Eq. (3) for the cases of internal dynamics (red points, left scale) and global diffusion (green triangles, right scale) of WSCP, respectively, as a function of Q^2 obtained from the fits shown in Fig. 3. The solid and dashed black lines are fits of the observed Q-dependence, see text for details.

decrease of elastic scattering at 0 meV with increasing Q and a concomitant increase of the quasielastic contribution.

The theoretical scattering function $S_{theor}(Q,\omega)$ used to fit the WSCP data is the convolution of $S_i(Q,\omega)$ describing internal protein dynamics and $S_g(Q,\omega)$ related to global diffusion of the protein under the assumption that both contributions are uncorrelated [20,21]:

$$\begin{aligned} S_{theor}(Q,\omega) &\cong S_i(Q,\omega) \otimes S_g(Q,\omega) \\ &= \frac{A(Q)}{\pi} \cdot \frac{\Gamma_g(Q)}{\omega^2 + \Gamma_g^2(Q)} \\ &\quad + \frac{1-A(Q)}{\pi} \cdot \frac{\Gamma_g(Q) + \Gamma_i(Q)}{\omega^2 + [\Gamma_g(Q) + \Gamma_i(Q)]^2} \cdot \end{aligned} \tag{3}$$

Before discussing the contributions $S_i(Q,\omega)$ and $S_g(Q,\omega)$, we note that the data in Fig. 3 are fitted by an experimental scattering function $S_{exp}(Q,\omega)$, which is the convolution of $S_{theor}(Q,\omega)$ with the experimentally obtained resolution function $R(Q,\omega)$. The resulting fits are shown as full lines in Fig. 3. Overall, the fit functions exhibit a very good agreement with the experimental data.

In more detail, the scattering function of global protein diffusion $S_g(Q,\omega) = \frac{1}{\pi} \cdot \frac{\Gamma_g(Q)}{\omega^2+\Gamma_g^2(Q)}$ generally accounts for both, translational and rotational diffusion of the protein approximated by a single Lorentzian with the half-width at half maximum (HWHM) $\Gamma_g(Q) = \hbar \cdot D_{\text{app}} \cdot Q^2$ where D_{app} is the apparent diffusion coefficient [22].

As to the internal protein dynamics of WSCP, the scattering function $S_i(Q,\omega)$ is given by [20,21]

$$S_i(Q,\omega) \cong A(Q) \cdot \delta(\omega) + \frac{1-A(Q)}{\pi} \cdot \frac{\Gamma_i(Q)}{\omega^2 + \Gamma_i^2(Q)}, \tag{4}$$

where the first and the second terms represent elastic and quasielastic scattering, respectively, $A(Q)$ is the elastic incoherent structure factor (EISF) and $\Gamma_i(Q)$ is the Lorentzian HWHM. The EISF obtained by fitting the WSCP spectra is shown as a function of scattering vector Q in the inset of Fig. 3. The EISF can be interpreted by the model for diffusion in a sphere according to [23]

$$A(Q) = p + (1-p) \cdot \left[\frac{3 j_1(QR)}{QR}\right]^2, \tag{5}$$

where j_1 is the first order spherical Bessel function, R is the radius of the sphere and p represents the immobile fraction of hydrogen atoms for a given resolution function. This model appears quite reasonable, because QENS probes the motions of small amino acid side groups confined by their environment. The fit reveals a radius of the sphere representing the confinement of $R = (2.7 \pm 0.3)$ Å and an immobile fraction of hydrogen atoms of $p = 0.50 \pm 0.03$. The latter value indicates that only about half of the hydrogen atoms of WSCP participate in motions on the investigated timescale.

The widths (HWHM) of the broad Lorentzian component corresponding to internal protein dynamics are shown in Fig. 4 (see red points) and exhibit a non-linear dependence on Q^2. The observed behaviour (for $Q^2 > 1$ Å^{-2}) can be well described by a jump-diffusion model (see full line in Fig. 4) given by $\Gamma_i = \hbar \frac{D_i Q^2}{1+D_i Q^2 \tau}$ [20], where D_i is the jump-diffusion coefficient and τ is the residence time before a jump. A constant value of $\text{HWHM}_{\text{internal}}$ at small Q may indicate a motion in confinement [21]. The fit shown in Fig. 4 yields a jump diffusion coefficient D_i of $(3.4 \pm 0.4) \cdot 10^{-5}$ cm^2/s and a residence time of $\tau = (1.2 \pm 0.2)$ ps. Both, the radius of the sphere R representing the confinement for the internal protein dynamics and the jump diffusion coefficient D_i obtained for internal WSCP dynamics compare favourably with the values reported by Stadler et al. [21] for haemoglobin in red blood cells.

Finally, we discuss the results gathered for global macromolecular diffusion of WSCP in D_2O buffer

solution. The widths of the narrow Lorentzian component are given by green triangles in Fig. 4. At the first glance, the widths of the narrow Lorentzian (HWHM) appear to be smaller than the Gaussian resolution of 0.123 meV (full width at half maximum). Nevertheless, this component turned out to be essential for proper fitting and cannot be omitted except for the smallest Q-value. Note in this regard the considerably larger error bar of the Lorentzian HWHM at the lowest Q-value. The reason for the observation of rather narrow widths most probably lies in the slow tailing of the Lorentzian function, so that its wings are visible even outside of the Gaussian resolution function. The linear increase of Lorentzian widths with increasing Q^2 is the signature of a continuous long-range (Brownian) diffusion of WSCP at 300 K. The slope of the linear fit shown in Fig. 3 corresponds to an apparent diffusion coefficient D_{app} of $(9.4 \pm 0.6) \cdot 10^{-7}$ cm^2/s. As expected, this value is significantly smaller than that of bulk water [24]. Recalling that D_{app} accounts for both, rotational and translational diffusion of WSCP, D_{app} has to be considered as an upper limit of the translational diffusion coefficient of WSCP.

4. Conclusions

We conclude that QENS studies on dynamics of proteins in buffer solution require a careful separation of buffer and protein contributions. As a result, WSCP dynamics can be reasonably modelled by two types of motion at room temperature: i) internal protein dynamics and ii) global diffusion of the whole WSCP molecule. Therefore, we anticipate that WSCP dynamics can be characterized by QENS over a larger temperature range, and WSCP can be used as an appropriate model system for studies of protein dynamics in photosynthetic pigment-protein complexes.

This work was supported by the European Social Fund's Doctoral Studies and Internationalisation Programme DoRa. We also thank for support by the Estonian Research Council (Grants ETF 9453, IUT 2-28 and SLOKT 12026 T), by the German Science Foundation (DFG, SFB 429, TP A1), and by PSI, Switzerland. L. R. and J. P. are grateful to the Scientific Exchange program under cooperation agreement between Estonian and Latvian Academies of Sciences for travel support. We also thank S. Kussin and M. Weß (TU Berlin) for their help during the H-D exchange procedure.

References

[1] J. Fitter, R.E. Lechner, N.A. Dencher, J. Phys. Chem. B **103**, 8036 (1999)
[2] J. Pieper, A. Buchsteiner, N.A. Dencher, R.E. Lechner, T. Hauß, Phys. Rev. Lett. **100**, 228103 (2008)
[3] W. Doster and M. Settles, Biochim. Biophys. Acta. **1749**, 173 (2005)
[4] J. Pieper, G. Renger, Photosynth. Res. **102**, 281 (2009)
[5] J. Pieper, T. Hauß, A. Buchsteiner, G. Renger, Eur. Biophys. J. **37**, 657 (2008)
[6] P. Kühn, J. Pieper, O. Kaminskaya, H.-J. Eckert, R. E. Lechner, V. Shuvalov, G. Renger, Photosyn. Res. **84**, 317 (2005)
[7] G. Renger, J. Pieper, C. Theiss, I. Trostmann, H. Paulsen, T. Renger, H.J. Eichler, F-J. Schmitt, J. Plant Phys. **168**, 1462 (2011)
[8] H. Satoh, A. Uchida, K. Nakayama, M. Okada, Plant Cell Physiol. **42**, 906 (2001)
[9] D. Horigome, H. Satoh, N. Itoh, K. Mitsunaga, I. Oonishi, A. Nakagawa, A. Uchida, J. Biol. Chem. **282**, 6525 (2007)
[10] C. Theiss, I. Trostmann, S. Andree, F. J. Schmitt, T. Renger, H. J. Eichler, H. Paulsen, G. Renger, J. Phys. Chem. B **111**, 46, 13325 (2007)
[11] F-J. Schmitt, I. Trostmann, C. Theiss, J. Pieper, T. Renger, J. Fuesers, H. Hubrich, H. Paulsen, H.J. Eichler, G. Renger, J. Phys. Chem. B **112**, 13951 (2008)
[12] J. Pieper, M. Rätsep, I. Trostmann, H. Paulsen, G. Renger, A., Freiberg, J. Phys. Chem. B **115** (14), 4042 (2011)
[13] J. Pieper, M. Rätsep, I. Trostmann, F-J. Schmitt, C. Theiss, H.J. Eichler, H. Paulsen, A., Freiberg, G. Renger, J. Phys. Chem. B **115** (14), 4053 (2011)
[14] Alster, J; Lokstein, H; Dostal, J; Uchida, A; Zigmantas, D, J. Phys. Chem. B **118**, 3524 (2014)
[15] J. Pieper, K-D. Irrgang, G. Renger, R.E. Lechner, J. Phys. Chem. B **108**, 10556 (2004)
[16] A. Gall, J., Seguin, B., Robert, M.-C. Bellissent-Funel, J. Phys. Chem. B **106**, 6303 (2004)
[17] S. Sacquin-Mora, P. Sebban, V. Derrien, B. Frick, R. Lavery, C. Alba-Simionesco, Biochemistry **46**, 14960 (2007)
[18] R.T. Azuah, L.R. Kneller, Y. Qiu, P.L.W. Tregenna-Piggott, C.M. Brown, J.R.D. Copley, and R.M. Dimeo, J. Res. Natl. Inst. Stan. Technol. **114**, 341 (2009)
[19] A. M. Gaspar, S. Busch, M. S. Appavou, W. Haeussler, R. Georgii, Y. X. Su, W. Doster, Biochim. Biophys. Acta Proteins Proteomics **1804**, 76, (2010)
[20] M. Bee, *Quasielastic Neutron Scattering: Principles and Applications in Solid State Chemistry, Biology and Materials Science* (Philadelphia, PA: Adam & Hilger, 1988)
[21] A.M. Stadler, L. van Eijck, F. Demmel, G.J. Artmann, R. Soc. Interface **8**, 590 (2011)
[22] J. Perez, J.M. Zanotti, D. Durand, Biophys. J. **77**, 454 (1999)
[23] F. Volino, A. Dianoux, J. Mol. Phys. **41**, 271 (1980)
[24] J. Pieper, G. Charalambopoulou, T. Steriotis, S. Vasenkov, A. Desmedt, R. E. Lechner, Chemical Physics (2003), 292, 465